



**HAL**  
open science

## Groundwater-surface water exchanges in an alluvial plain in southern France subjected to pumping: A coupled multitracer and modeling approach

Jérôme Texier, Julio Gonçalves, Thomas Stieglitz, Christine Vallet-Coulomb, Jérôme Labille, Vincent Marc, Angélique Poulain, Philippe Dussouillez

### ► To cite this version:

Jérôme Texier, Julio Gonçalves, Thomas Stieglitz, Christine Vallet-Coulomb, Jérôme Labille, et al.. Groundwater-surface water exchanges in an alluvial plain in southern France subjected to pumping: A coupled multitracer and modeling approach. *Journal of Hydrology: Regional Studies*, 2024, 56, pp.101995. 10.1016/j.ejrh.2024.101995 . ird-04757488

HAL Id: ird-04757488

<https://ird.hal.science/ird-04757488v1>

Submitted on 29 Oct 2024

**HAL** is a multi-disciplinary open access archive for the deposit and dissemination of scientific research documents, whether they are published or not. The documents may come from teaching and research institutions in France or abroad, or from public or private research centers.

L'archive ouverte pluridisciplinaire **HAL**, est destinée au dépôt et à la diffusion de documents scientifiques de niveau recherche, publiés ou non, émanant des établissements d'enseignement et de recherche français ou étrangers, des laboratoires publics ou privés.



Distributed under a Creative Commons Attribution 4.0 International License

# Groundwater-Surface water exchanges in an alluvial plain in southern France subjected to pumping: a coupled multitracer and modeling approach

Jérôme Texier<sup>a</sup>, Julio Gonçalves<sup>a</sup>, Thomas Stieglitz<sup>a</sup>, Christine Vallet-Coulomb<sup>a</sup>, Jérôme Labille<sup>a</sup>,  
5 Vincent Marc<sup>b</sup>, Angélique Poulain<sup>b</sup>, Philippe Dussouillez<sup>a</sup>

<sup>a</sup> Aix Marseille Univ, CNRS, IRD, INRA, Coll France, CEREGE, 13545, Aix-en-Provence, France

<sup>b</sup> UMR EMMAH Environnement Méditerranéen et Modélisation des Agro-Hydrosystèmes, University of Avignon, 84000 Avignon, France

*Correspondence to:* Jérôme Texier (texier@cerege.fr)

## 10 **Abstract**

### Study Region:

The study was conducted in an alluvial plain between the Rhône and the Ouvèze Rivers (in the southeast of France) extensively exploited for drinking water. The research area is characterized by significant groundwater-surface interactions influenced by groundwater pumping activities.

### 15 Study Focus:

The aim of this study is to enhance the understanding of interactions between rivers and alluvial aquifers by combined multi-tracer and numerical modeling approaches. Over an 18-month period, groundwater temperature, piezometric levels, and river surface water levels were continuously monitored. Field campaigns focused on conductivity, stable isotopes of water, and radon-222 activity concentration in both groundwater and surface water. Radon-222 was used to quantify water exchanges  
20 between the river and the aquifer. A MODFLOW model, calibrated using piezometric data and PEST, was employed to simulate groundwater flow and reactive transport of radon-222 using MT3DMS.

### New Hydrological Insights for the Region:

The study reveals that river water recharges the aquifer, with radon-222 data delineating this recharge zone. The methodology extended the interpretation of periodic groundwater temperature signals to isotopic signals, allowing the identification of  
25 dispersivity and Darcy's velocity. The Ouvèze River was found to contribute approximately 55% of the pumping water supply, alongside the Rhône. These findings provide valuable insights for sustainable water resource management, demonstrating the relevance of using natural tracers in scenarios where artificial tracers are impractical.

## **Keywords**

Alluvial aquifers, River-aquifer interactions, Multi-tracer approach, Numerical modelling, Groundwater recharge, Radon-222  
30 tracers, Stable isotopes, MODFLOW model, Rhône River, Ouvèze River, Groundwater temperature monitoring, Water resource management, Sustainable water management, Hydrological study

# 1 Introduction

When surface water and groundwater are connected, the abstraction of one of them can impact both resources and their interactions. Modifying the direction and/or rates of their respective exchange fluxes can influence the long-term quantity and quality of surface water and groundwater (Lu et al., 2018; Shu and Chen, 2002; Sophocleous, 2002; Winter, 1999; Winter et al., 1999), affecting ecosystem equilibrium (Woessner, 2000), and downstream users (Winter et al. 1998). Alluvial aquifers hydraulically connected to rivers are widely exploited and represent a major water resource. Although the proximity to the river can ensure significantly high aquifer pumping rates, water quality problems can be encountered for those pumping fields along the riverbanks (Bertln and Bourg, 1994; Hiscock and Grischek, 2002). Quantifying groundwater-surface water exchange is essential for understanding and joint management of surface water and groundwater resources (Fleckenstein et al., 2010; Shanafield and Cook, 2014), as well as for possible contamination management (Boano et al., 2010; Chapman et al., 2007; Chen, 2007; Lamontagne et al., 2005; Trauth et al., 2018).

The characterization of groundwater-surface water exchanges as well as methods to describe them, both in quantitative and qualitative terms has been widely studied (Bernard-Jannin et al., 2017; Lu et al., 2018; Brunner et al., 2009; Rivière et al., 2014; Cardenas, 2009). Quantification of exchange is generally based on differential gauging or Darcy flow estimates using piezometric records and hydraulic conductivity values (Dujardin et al., 2014; Keery et al., 2007; Schmidt et al., 2007; Xie et al., 2016). However, estimates of Darcy flows based on piezometric level data are difficult due to problems in obtaining reliable hydraulic heads and hydraulic conductivity from piezometers, especially in the case of a riverbed and due that it is integrative in space (Keery et al., 2007; Surridge et al., 2005). In addition, the hydraulic conductivity of riverbed sediments is likely to vary by several orders of magnitude in space (Calver, 2001), adding further uncertainty to the Darcy flux estimates. Differential gauging corresponding to river flow measurement at different location of the river to determine gains or losses linked to the connection with the aquifer. This method is commonly used to estimate groundwater-surface water exchange flow at the watershed scale and allows reliable and inexpensive measurement and is generally applied to rivers with low to moderate discharge (from  $0.001 \text{ m}^3 \text{ s}^{-1}$  to  $500 \text{ m}^3 \text{ s}^{-1}$ ; (Grapes et al., 2005; Konrad, 2006; McCallum et al., 2012; Opsahl et al., 2007; Xie et al., 2016). However, its application becomes challenging for high flow rivers like the Rhone, necessitating fixed gauging stations rather than manual flow measurements (Konrad, 2006; Xie et al., 2016).

Artificial tracers are chemical compounds not naturally present in the water and cannot always be used due to large river discharge or to the proximity to sensitive sites (industrial, urban), so the use of natural tracer has been widely developed. Thermal signal transfer is a relevant tool for assessing water transfers from rivers to unconfined aquifers that has attracted great attention over the past two decades (Constantz, 2008; Keery et al., 2007). The advantage of temperature as a tracer, compared to hydraulic approaches, is that thermal properties vary less than hydraulic properties, such as hydraulic conductivity, thus reducing the uncertainty of exchange flux estimates (Boano et al., 2010; Lautz, 2010). The interest of temperature monitoring relies on its ease of implementation with inexpensive data loggers, even over relatively long times and with fine time resolution (Constantz, 2008; Constantz and Stonestrom, 2003; Keery et al., 2007). Most studies focus on vertical

65 temperature transfer from the river to the aquifer at the riverbed (Anderson, 2005; Constantz, 2008; Ghysels et al., 2021; Rosenberry et al., 2016; Xie and Batlle-Aguilar, 2017). Exchange fluxes are then estimated, by fitting an analytical solution to vertical riverbed temperature profiles (Constantz, 2008; Schmidt et al., 2007), by analyzing time series of temperature data (Anibas et al., 2011; Rosenberry et al., 2016), or by means of coupled modeling of groundwater flow and heat transport (Anibas et al., 2011; Schmidt et al., 2007). Temperature is rarely used directly to quantify lateral (horizontal) exchange between streams and aquifers but can be used as a calibration variable to constrain numerical models (Bravo et al., 2002; Brookfield and Sudicky, 2013; Tang et al., 2017). In these cases, piezometers and temperature sensors are often installed near the river (Engelhardt et al., 2011; Gerech et al., 2011; Musial et al., 2016).

Along with temperature, the use of radon-222 isotope is considered one of the most effective and well-established tracing techniques in hydrogeological studies (Kurylyk et al., 2018; Rau et al., 2010; Ren et al., 2018). This natural radioactive tracer is generally used to quantify the groundwater flow towards surface bodies such as coastal lagoons or rivers (Cook et al., 2018, 2006; Dugan et al., 2012; Hoehn and Von Gunten, 1989; Stellato et al., 2008; Stieglitz et al., 2013, 2010). Radon-222 is a naturally occurring gaseous radioactive isotope with a short half-life (3.8 days). In groundwater, the activity concentration of radon-222 is high, because it is produced by the decay of radium present in the soil minerals (Kraemer et al., 1998). Surface waters generally have low radon-222 activity concentrations due to the negligible radon-222 content in precipitation, outgassing in the water column, and its short radioactive half-life (Bertln and Bourg, 1994; Cecil and Green, 2000; Cook et al., 2006; Dugan et al., 2012). This difference allows for radon-222 to be used as a tracer of groundwater discharge to surface water bodies (Hoehn and Von Gunten, 1989; Mayer et al., 2018; Stellato et al., 2008). Radon-222 mass balance calculations enable the quantification of radon-222 and therefore groundwater fluxes upon quantification of radon-222 concentration in groundwater (Cable et al., 1996; Cook et al., 2006; Corbett et al., 1997; Ellins et al., 1990). However, the situation of a losing river, i.e., surface water supplying the groundwater is less studied. In this situation, it is possible to obtain qualitative information on surface water groundwater exchange, when the boreholes are close to the river, and quantitative information, such as velocity and transit time, by analyzing the continuous radon-222 record (Close et al., 2014; Hoehn and Von Gunten, 1989).

Stable isotopes of water ( $^{18}\text{O}$  and  $^2\text{H}$ ) are commonly used as conservative tracers in hydrology. Isotopic methods rely primarily on the Meteoric Water Line (MWL), which expresses a linear relationship between  $\delta^2\text{H}$  and  $\delta^{18}\text{O}$  values due to isotopic fractionation during condensation of water vapor mass (Craig, 1961; Clark and Fritz, 1997) and represents the natural variations of the meteoric water composition before the influence of post-precipitation evaporation processes. The isotopic composition of groundwater has been widely used to determine the origins of groundwater recharge, estimate mixing proportions between different sources, quantify recharge rates (Clark and Fritz, 1997; Engelhardt et al., 2011; Fette et al., 2005; Gat et al., 1969; Gonçalves et al., 2015; Séraphin et al., 2016; Sharma and Hughes, 1985; Vallet-Coulomb et al., 2017). The application of stable water isotopes also makes it possible to improve numerical modeling of groundwater-surface water interactions, in particular by distinguishing different sources of water or by evaluating the recharge (Binet et al., 2017; Long and Putnam, 2004; Perrin et al., 2003). Especially when contrasted signatures can be identified between a river and its accompanying alluvial

aquifer, as is the case for rivers fed at high altitude, the application of stable isotopes of water also makes it possible to trace the surface water – groundwater exchanges and to determine the transit times (Poulain et al., 2021a, 2021b).

Tritium ( $^3\text{H}$ ) is another valuable tracer that could have been considered for this study, particularly due to the presence of nuclear power plants along the Rhône River, which release tritium at relatively high concentrations into the surface water. Tritium, with its longer half-life of approximately 12 years, has been used effectively in previous studies to investigate groundwater-surface water interactions, as demonstrated by e.g. Engel et al. (2024), Zill et al. (2023), and Schubert et al. (2020). However, this study focused on natural tracers that are less influenced by anthropogenic sources, with the aim of understanding the natural dynamics of river-aquifer interactions and to explore methods that could be broadly applicable in other regions where tritium may not be as prevalent or where nuclear facilities are absent.

The integration of spatial and temporal data from field and laboratory experiments with physically based numerical models is a current focus of research. This approach assists in uncovering important dynamics and enhances our comprehension of various processes. (Binet et al., 2017; Fleckenstein et al., 2010; Ghysels et al., 2021; Gilfedder et al., 2015; Jiang et al., 2019). Regarding groundwater-surface water exchanges, regional studies most often use MODFLOW type models with rivers represented by Cauchy type or prescribed hydraulic head boundary conditions (Cousquer et al., 2017; Di Ciacca et al., 2019; Morel-Seytoux et al., 2018, 2014; Rushton, 2007). However, calibration does not guarantee the reliability of a model, indeed several problems can arise as the possibility of multiple parameterizations (recharge, steady state hydraulic conductivity) to obtain the same result, the so-called equifinality issue (Bravo et al., 2002; Cousquer et al., 2018, 2017). In this context, the acquisition of constraining data (e.g., tracers) to increase the reliability of the variables and parameters (hydraulic conductivity, recharge, dispersivity...) is fundamental to improve the model quality (Cousquer et al., 2018; Delottier et al., 2017; Fleckenstein et al., 2010; Gardner et al., 2011). Although tracers can be individually used, the information obtained by combining different techniques (tracers) can validate the results and overcome the limitations of a single method (Dujardin et al., 2014; Gardner et al., 2011; Gilfedder et al., 2015; Sadat-noori et al., 2021; Stellato et al., 2008; Xie et al., 2016).

In this study, we combined a multitracer approach and numerical modeling to quantify the groundwater-surface water interactions at the local scale, in the context of groundwater exploitation by riverside pumping. A catchment field located on the banks of the Rhône River, in southeastern France, was chosen as the study site. This site has the particularity of being located between two rivers (Rhône and Ouvèze), thus likely prescribing hydraulic head values at river stages on each side if the rivers are connected to the exploited aquifer. As the pumping wells are located only a few dozen meters from the Rhône, there is a risk of pollution by the river. The main aim of this study is to accurately determine the origin and proportions of the various water sources feeding a well system on an alluvial plain. This study needs the following steps:

- i) Identification of the water sources feeding the pumping wells using at least two distinct tracers (radon-222 and stable water isotopes) and the piezometric data (hydraulic head (m));
- ii) Analysis of temperature seasonality in the piezometers and Rhône River to estimate pore velocity ( $u$ ), based on known porosity;
- iii) Use of  $\delta^{18}\text{O}$  seasonality in piezometers to constrain dispersivity, a crucial but often poorly known property;

iv) The use of steady-state flow modelling coupled with reactive transport (radon-222 with radioactive decay) to confirm the origins and determine the proportions of the pumped water mixture, using pore velocity and radon-222 signal for model validation.

Through these steps, the study aims to provide a comprehensive understanding of water dynamics in the alluvial plain, essential for sustainable management of water resources.

Piezometers and pumping wells were equipped with pressure and temperature sensors. In addition to continuous piezometric monitoring, various methods of evaluating the water exchanges between the alluvial aquifer and the river were implemented to obtain robust information on the nature and direction of the flows. The transfer of the seasonal (periodic) temperature signal from the Rhône River to the aquifer was monitored to quantify the lateral water exchange as well as the thermal diffusivity of the aquifer (measure of how heat flow occurs within the material). Several radon-222 and electric conductivity measurement campaigns were carried out to determine the nature of the exchanges in different operating situations (pumping or no pumping). The temporal monitoring of stable isotopes of water allows us to identify the different sources of water supplying the pumping wells and to characterize the mixing. By transposing the thermal periodic signal interpretation method and thus its analytical solution to the mass transfer problem, the stable isotopes of water time series analysis could enable quantifying the dispersivity of the medium. These different methods lead to a comprehensive understanding of the hydrodynamic behavior of the aquifer in a robust and repeatable way in the very common context of groundwater exploitation in an alluvial plain. All these data were aggregated and used to constrain a local hydrogeological model using MODFLOW and highlighting the vulnerabilities of the site regarding possible contamination coming from the rivers.

To our knowledge, we propose several new approaches to improve our understanding of alluvial aquifers in the context of river-groundwater exchange. While radon-222 is conventionally used for estimating groundwater discharge in rivers, it has been employed here to determine water flow from river to aquifer, characterized by the dilution of the aquifer's natural radon-222 signal by radon-depleted river waters. Previous studies typically focus solely on either gaining river or losing river scenarios. However, it is uncommon to altern gain/losing scenarios at the same site. This unique situation, made possible by an exceptional cessation of pumping, facilitated the efficient use of radon-222 to identify the origin and proportions of the water supplying the pumping wells. To our knowledge, the use of radon-222 data in transport models is also rarely discussed and represents a further addition to improve and constrain numerical models. In addition, we propose an extension of the standard 1D interpretation of the periodic temperature signal to the periodic signal of stable water isotopes. Interpreting a natural tracer such as stable isotope of water, in the context where the use of artificial tracers is not feasible, theoretically allows assessing the poorly known dispersivity of the alluvial aquifer.

## 2 Study site, material and method

### 165 2.1 Field Site

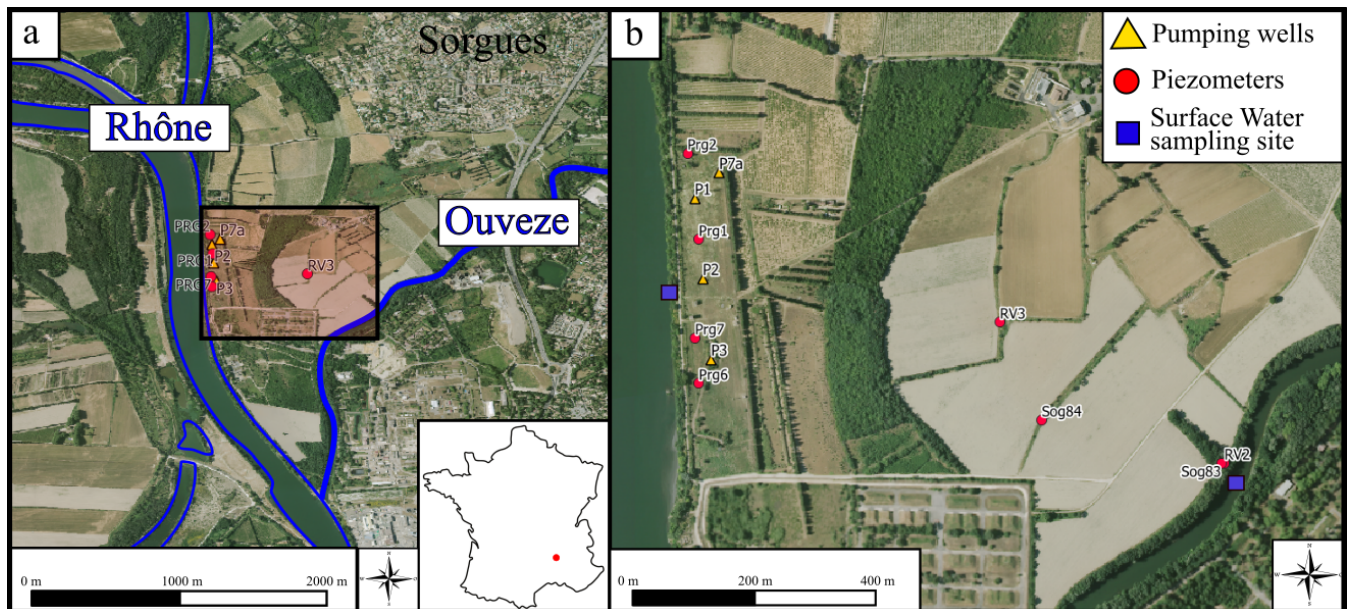


**Figure 1 :** a) Map of the study area the Jouve site (Vaucluse, France) located in the red inset b) the monitored pumping wells and piezometers symbolized by yellow triangles and red points respectively. The water surface sampling sites are symbolized by blue squares (© Google Earth 2022).

170 The study site located at Sorgues (Vaucluse, Southeast of France, Figure 1) is the domestic water extraction site of La Jouve  
composed of pumping wells aligned along the Rhône riverbanks. The pumping site is located upstream of the confluence of  
the Rhône (average monthly flow rate;  $400 \text{ m}^3 \text{ s}^{-1}$ ) and Ouvèze (average monthly flow rate;  $20 \text{ m}^3 \text{ s}^{-1}$ ). These two important  
surface water bodies result in a great local stability of groundwater levels. The site is equipped with piezometers allowing the  
monitoring of the water table and of four active pumping wells operating intermittently for a total extraction flow of  $11,000 \text{ m}^3$   
175 per day. The exploited unconfined alluvial aquifer corresponds to a plio-quaternary formation mainly composed of sand and  
pebbles deposited by the Rhône River. The aquifer substratum at the extraction site is composed of Miocene blue marls from  
between an elevation of 9 and 11m absl(Caridroit, 1968; Nofal, 2014). For the Rhône, the level is controlled upstream at the  
northwest by the Sauveterre dam which maintains the river stage at about 16.5 m absl.

### 2.2 Material

180 The pumping wells (P1, P7A, P3; see Figure 1) were equipped with temperature sensors (HOBO Water Temp Pro v2) in  
February 2019. The groundwater level of the pumping wells being provided by the pumping wells operator. The accuracy,  
resolution and response time of the probes are  $0.2 \text{ }^\circ\text{C}$ ,  $0.02 \text{ }^\circ\text{C}$  and 5 min, respectively. Four piezometers on the pumping site,  
and one outside (200 m to the East, RV3 see Figure 1), have been also equipped with pressure and temperature sensors (OTT

Orpheus Mini) with an accuracy of 0.05% for water-level measurement and a resolution of 0.1 °C and an accuracy of 0.5 °C  
185 for temperature. The temperature and the river stage of the Rhône were also monitored. All probes have been configured to  
record measurements every 15 minutes.

Radon-222 sampling was conducted in surface water and groundwater during three campaigns: March 2020, June 2020, and  
April 2021. The first campaign focused on the Rhône riverbank and the pumping site during a period of pumping shutdown.  
The second occurred when pumping activity resumed and focused on the groundwater abstraction site. The third campaign  
190 focused on the Ouvèze riverbank and the aquifer outside the site in the same hydrodynamic context of the second campaign  
(pumping wells functioning and related pseudo-steady state). The radon-222 activity concentration of the samples was  
measured at the laboratory using electronic radon-in-air monitors DurrIDGE RAD-7 coupled with the DurrIDGE RAD H2O  
system,. The RAD H2O system uses a closed-loop air stripping method to transfer radon from the water sample into a  
measurement cell, where the radon concentration is then quantified using a RAD7 detector (Schmidt et al., 2010). The monitors  
195 count  $\alpha$  decays of radon-222 progeny, and radon-222 activity concentration is determined by discriminating  $^2$ radon-222  
progeny decays in specific energy windows. The radon-222 activity concentration in water is then calculated from the activity  
concentration measured in air with a known temperature correlation (Weigel, 1978). During the campaign additional electric  
conductivity measurements were made for all radon-222 samples with a multimeter field sensor.

Surface water and groundwater were collected between June 2019 and November 2020 for water stable isotope analysis ( $^{18}\text{O}$ ,  
200  $^2\text{H}$ ). Groundwater samples were collected in the pumping wells and piezometers by means of a submersible groundwater pump  
and access taps. For the piezometer a pumping time equivalent to the displacement of 3 borehole volumes (calculated using  
the borehole geometry and the piezometric levels) resulted in a constant value of electric conductivity (measured during  
sampling with a multimeter field sensor). The composition in  $\delta^{18}\text{O}$  and  $\delta^2\text{H}$  of the water samples were analyzed using a  
Picarro L2140-i wavelength-scanned cavity ring-down spectroscopy (CRDS), following the protocols described in Vallet-  
205 Coulomb et al. 2021 for post-measurement data processing. All samples were filtered at 0.45 $\mu\text{m}$  before analysis and analyzed  
twice. All data are provided in ‰ vs VSMOW, after normalization to the VSMOW2-VSLAP scale. Based on the performances  
obtained for samples of a laboratory standard included in each analysis runs as a quality assurance / quality control, the  
precision obtained was 0.03‰ and 0.09‰ for  $\delta^{18}\text{O}$  and  $\delta^2\text{H}$  respectively (n = 6 runs). The Rhône isotopic signature records  
were obtained by the Avignon databases (Poulain et al., 2021b, 2021a).

## 210 **2.3 Methodological approaches**

### **2.3.1 1D temperature analysis**

Heat transfer in a half-space (river infinite porous medium) is assumed to be governed by a one-dimensional conduction-  
advection equation, i.e. considering both the heat transfer due to water convection and heat conduction through the solid and the  
liquid phases. This equation is usually solved in the framework vertical transfers from the streambed downwards (Hatch et al.,  
215 2006; Stallman, 1965) (1).



$$\frac{\partial T}{\partial t} = Ke \frac{\partial^2 T}{\partial z^2} - \frac{nv_f}{\gamma} \frac{\partial T}{\partial z} \quad (1)$$

where  $T$  is temperature ( $^{\circ}\text{C}$ ) variable with time  $t$  (s), and depth  $z$  (m),  $Ke$  is the effective thermal diffusivity ( $\text{m}^2 \text{s}^{-1}$ ),  $\gamma = \frac{\rho c}{\rho_f c_f}$  the ratio of the heat capacity (-) of the streambed to that of the fluid,  $n$  is the kinematic porosity (-), and  $v_f$  is the vertical fluid velocity  $\text{m.s}^{-1}$ .

- 220 The heat transfer from the Rhône River to the aquifer was studied by adapting the one-dimensional (1D) solution to calculate the amplitude change of a periodic temperature signal (seasonal signal of the surface water) with the distance to the riverbed and the shift when this signal is propagating within the aquifer (Goto and Matsubayashi, 2009; Stallman, 1965). This analytical solution, in its standard form, assumes 1D uniform vertical flow, sinusoidal behavior of the surface temperature, and no change in the average temperature with depth of the response time to the temperature variation at the surface (Hatch et al., 2006).
- 225 However, applying this solution can become challenging in the presence of complex thermal signals in the river or non-constant flow rates. In such cases, the best alternatives are numerical models based on finite differences or finite elements schemes that simulate heat transport in porous media. These models, although more sophisticated, are less accessible due to their complexity and the need for specialized expertise in numerical modeling. (Munz and Schmidt, 2017). Here, the solutions of Goto (2005) and Stallman (1965) have been adapted to study the attenuation and phase shift in the case of a purely horizontal ( $x$ -axis)
- 230 transfer from a riverbank and writes (2). An inversion using the temperature records of the piezometers allows quantification of two parameters: the flow velocity and the effective thermal diffusivity of the alluvial aquifer using the following expression:

$$T(x, t) = A \exp\left(\frac{vx}{2Ke} - \frac{x}{2Ke} \sqrt{\frac{\alpha + v^2}{2}}\right) \cos\left(\frac{2\pi t}{P} - \frac{x}{2Ke} \sqrt{\frac{\alpha - v^2}{2}}\right) \quad (2)$$

- where  $A$  is the amplitude of the temperature variations (-),  $P$  is the period of temperature variations (s),  $v$  is the horizontal
- 235 velocity ( $\text{m.s}^{-1}$ ) and  $\alpha = \sqrt{v^4 + \left(\frac{8\pi Ke}{P}\right)^2}$

### 2.3.2 1D Stable isotope transport

The lateral transfer of surface water into the alluvial aquifer can also be studied using the periodic signal of the stable isotopes of water. For this purpose, the sinusoidal fluctuations of the isotope concentration can be studied by adapting to mass transport the previous solution for heat transfer. By parameter identification of the 1D dispersion advection equation (3) which writes:

240 
$$\frac{\partial C}{\partial t} = D \frac{\partial^2 C}{\partial x^2} - v_f \frac{\partial C}{\partial x} \quad (3)$$

and heat transfer equation (1), the analytical equation (2) was transposed to a mass transport problem giving (4):

$$C(x, t) = A \exp\left(\frac{v_f x}{2D} - \frac{x}{2D} \sqrt{\frac{\alpha + \frac{v_f^2}{n}}{2}}\right) \cos\left(\frac{2\pi t}{P} - \frac{x}{2D} \sqrt{\frac{\alpha - \frac{v_f^2}{n}}{2}}\right) \quad (4)$$

Eq. (4) was applied on the stable of water monitoring. Using the Darcy velocity obtained from temperature signal interpretation (eq. 2), eq. 4 allows identifying the dispersion coefficients (D).

245

### 2.3.2 Coupled Flow and Radon-222 Transport Model

In order to integrate piezometric and radon-222 data to estimate the site's vulnerability to contamination and quantify sources, a model was built using MODFLOW. The numerical codes used for groundwater flow and transport modeling are MODFLOW (McDonald and Harbaugh, 1988) for groundwater flow and MT3DMS (Zheng and Wang, 1999) for advective-dispersive  
 250 transport integrated into the PROCESSING MODFLOW X software. MODFLOW solves the diffusivity equation using a finite difference method. Thus, for horizontal 2D flows in a free, heterogeneous and isotropic aquifer, the diffusivity equation writes:

$$\omega_s \frac{\partial h}{\partial t} + Q(x, y) = \frac{\partial}{\partial x} \left( T(x, y) \frac{\partial h}{\partial x} \right) + \frac{\partial}{\partial y} \left( T(x, y) \frac{\partial h}{\partial y} \right) (5)$$

With  $\omega_s$  (-) the specific yield,  $h$  (m) the hydraulic head,  $T(x, y)$  ( $\text{m}^2 \text{s}^{-1}$ ) the aquifer transmissivity,  $Q(x, y)$  ( $\text{m} \text{s}^{-1}$ ) source or sink term.

255 MT3DMS was used for radon-222 transport calculations. MT3DMS allows the simulation of dissolved species concentrations by considering advection, dispersion, molecular diffusion, and chemical reaction (Zheng et al., 2012; Zheng and Wang, 1999). MT3DMS thus relies on the flow solutions of MODFLOW to solve the advection-dispersion equation:

$$\frac{\partial(\theta C)}{\partial t} = \frac{\partial}{\partial x_i} \left( \theta x_{ij} \frac{\partial C}{\partial x_j} \right) - \theta v_i \frac{\partial C}{\partial x_i} + q_s C_s + \sum R_n (6)$$

where  $C$  ( $\text{kg m}^{-3}$ ) the concentration of the dissolved species,  $\theta$  (-) the aquifer porosity,  $x_i$  (m) the distance belong an axe,  
 260  $D_{ij}$  ( $\text{m}^2 \text{s}^{-1}$ ) the dispersion coefficient,  $v$  ( $\text{m s}^{-1}$ ) the pore velocity,  $q_s$  ( $\text{s}^{-1}$ ) the volumetric flow rate per unit volume of the source or sink,  $\sum R_n$  ( $\text{g m}^3 \text{s}^{-1}$ ) the chemical reactions term.

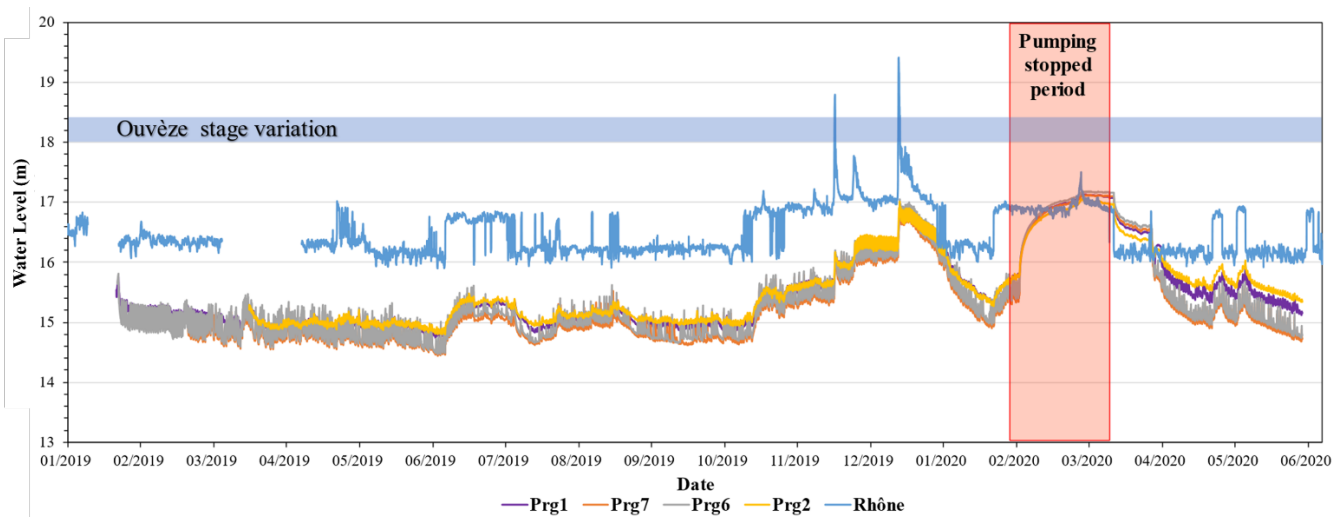
The modeled surface area is 3  $\text{km}^2$  and covers the Jouve site and the two rivers, the Rhône and the Ouvèze. The boundary conditions (BC) of the model are prescribed hydraulic head conditions: the Rhône at the western limit set at 16.5 m, the Ouvèze at the east set at 18.2 m and a northern limit at 17 m, considered time invariant according to the piezometric monitoring of the  
 265 pumping field operator. The northern BC is set at 17 m by analysis of previous operator piezometric maps indicating a zone around 17 m due to the influence of the Rhône and Ouvèze rivers on the alluvial groundwater table. Unfortunately, there is no geological boundary in the vicinity that could be used as an alternative BC. The model is composed of 2600 rows and 2200 columns with 5m wide grid cells. The model includes one aquifer layer limited by a lower surface corresponding to the alluvial substratum and an upper surface corresponding to the topography. An annual recharge of 300 mm years by direct rainwater  
 270 infiltration was introduced based on previous estimates in the Avignon region (Nofal, 2014). The hydraulic conductivity field is considered heterogeneous, so the study area was divided into 10 zones, each with a constant hydraulic conductivity to becalibrate. The calibration to adjust the hydraulic conductivity field of the model to reproduce the measured piezometric levels (10 observations points) was performed at steady-state using the PEST suit, a standard gradient-based optimization algorithm (Doherty, 2004). Initial hydraulic conductivity values were obtained by interpolation using data from the operator's

275 hydraulic test reports (value of  $1.10^{-2}$  to  $1.10^{-4}$  m s<sup>-1</sup>). Radon-222 transport was integrated into the model by including the  
radioactive half-life of radon-222 (3,823 days) in MT3D and by setting the rivers at a constant concentration of radon-222  
measured ( $0.2 \text{ Bq L}^{-1}$ ). This value of  $0.2 \text{ Bq L}^{-1}$  is consistent with the measurement campaign with radon-222 activity  
concentration in both rivers ranging between 125 and 225 Bq/m<sup>3</sup>. A dispersivity of 10 meters was used based on usually found  
values in the literature for sandy alluvial aquifers at this scale (Schulze-Makuch, 2005). The aquifer radon-222 source term,  
280 representing the background radon-222 concentration, was determined by simulating the natural production of radon-222  
within the aquifer material. This was conveniently achieved using the flow injection wells package in MODFLOW, where  
each cell of the aquifer was assigned a low, uniform injection rate (to avoid impacting the piezometric levels) at a constant  
radon-222 concentration. The concentration of radon-222 injected were uniformly applied given the lack of specific  
information on geological heterogeneities. These parameters were then calibrated using the PEST software to best match the  
285 observed radon-222 activity concentrations in the aquifer. This approach allowed to reproduce the natural radon-222  
production and ensure that the model reflects the measured radon-222 activity concentration.

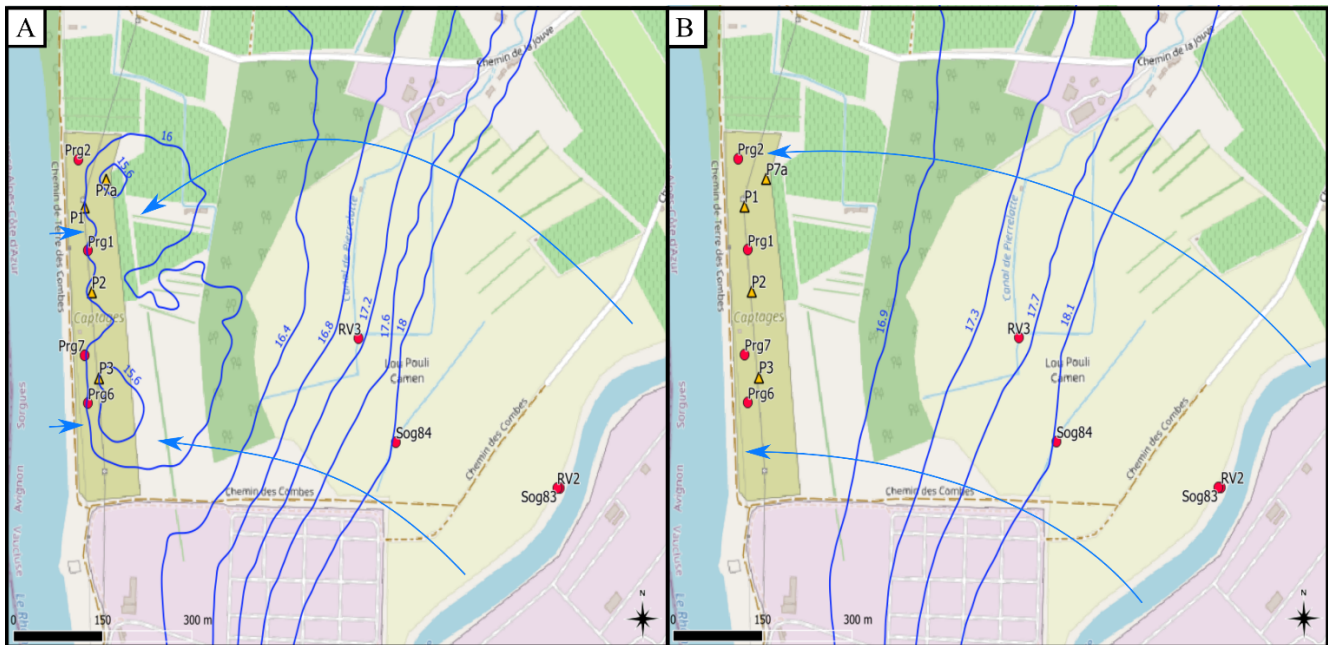
### 3 Results

#### 3.1 Piezometric level variations

290 The daily piezometric level variations at the site (Figure 2) are controlled by the pumping cycles of the four wells (P1, P2, P3  
and P7A). Over a period of continuous pumping, from January 2019 to February 2020, the pumping maintains the water level  
between 15.5 m and 14.6 m, except during flooding events of the Rhône River. A pseudo-steady state is therefore established  
at the site caused by periodic pumping. River stage variations of the Rhône influence the water table, particularly during  
periods of flooding marked by a sharp increase in the level of the Rhône (Figure 2). When the site is operative, the water table  
is permanently below the Rhône River stage, even during short pumping stops and floods. The conditions are therefore  
295 favorable for an exchange from the Rhône to the alluvial aquifer (Figure 3A). During periods of flooding, the Rhône River  
rises to an average value of 16.9 m. Higher values were observed in October and December 2019 with sharp increases to  
18.9 m and 19.4 m respectively as a result of water releases from the Sauveterre dam (Figure 2). Site maintenance operation  
led to a prolonged pumping stop (6 weeks during spring 2020, red period, Figure 2). During this period, the water table rose  
300 progressively until reaching a stable level above the Rhône River stage, and the exchanging flow between the Rhône and the  
alluvial aquifer likely reversed. This case corresponds to the natural hydraulic condition leading to a flow from the Ouvèze to  
the Rhône (Figure 3B). The connection between the alluvial aquifer and the Ouvèze is suggested by the piezometric map but  
requires further confirmation in the following sections.



305 **Figure 2 : Piezometric level time series at the study site of la Joue (Prg1, Prg7, Prg6, Prg2) and Rhône River stage time series at 15 min intervals.**



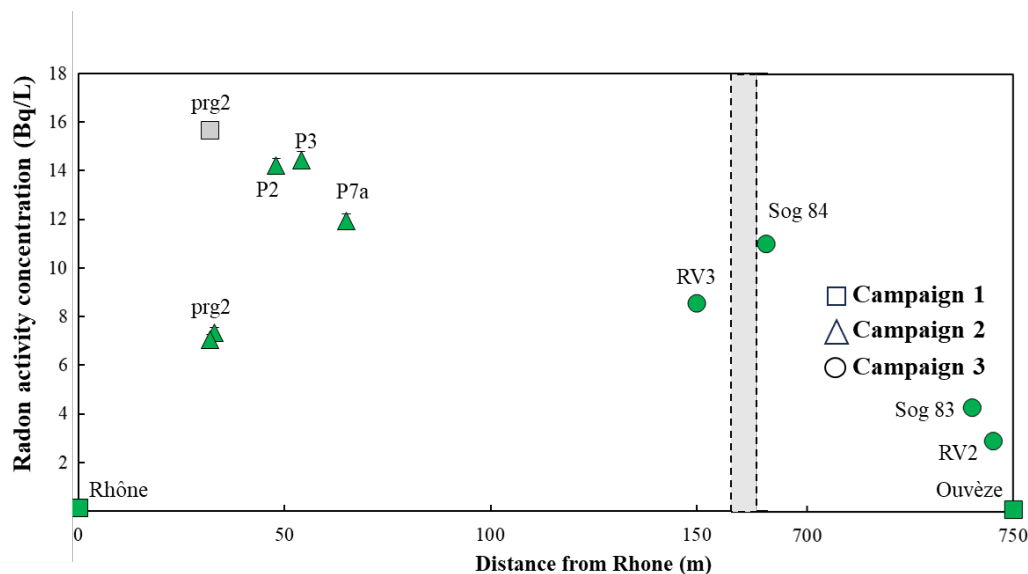
310 **Figure 3 : A) Piezometric map obtained by interpolation of piezometric level using the inverse distance to a power method (campaign during October 2018). B) Piezometric map obtained by interpolation of piezometric level using the inverse distance to a power method (Pumping Stopped March 2020). © OpenStreetMap contributors 2022. Distributed under the Open Data Commons Open Database License (ODbL) v1.0.**

### 3.2 Radon-222 and Electrical conductivity data

During the first field campaign, when the pumping wells were stopped, the radon-222 signature of the Rhône was about  $0.2 \pm 0.03 \text{ Bq L}^{-1}$  and at the Prg2 piezometer, the value was at  $15 \pm 0.35 \text{ Bq L}^{-1}$  (Figure 4). During the second campaign, pumping

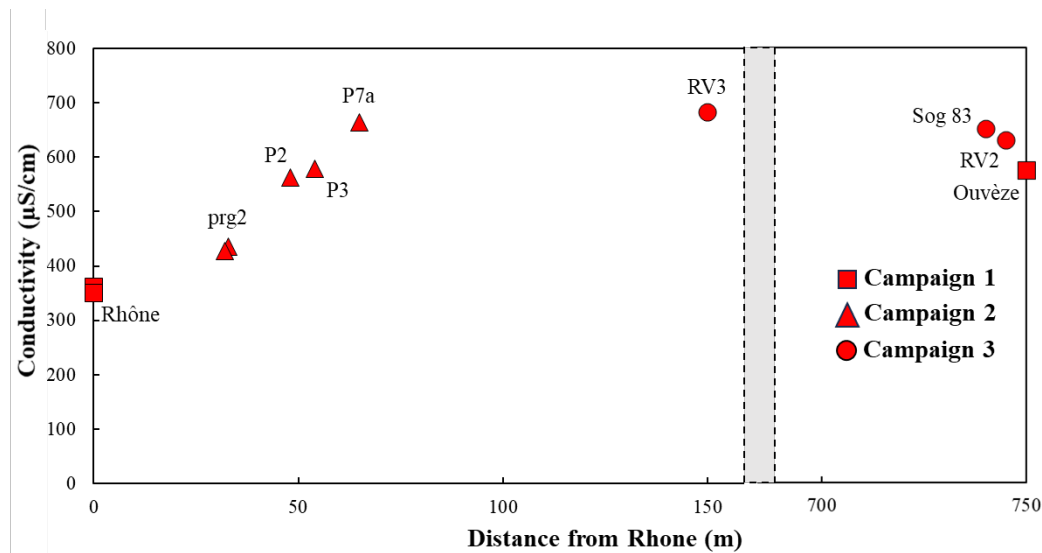
315 was restored and the usual piezometric levels were recovered; the same piezometer, Prg2, showed radon-222 activity concentrations four times lower at  $3.0 \pm 0.24 \text{ Bq L}^{-1}$ . The other piezometers, close to the Rhône, showed similar low values, while the pumping wells further away were at values of between  $10.0 \text{ Bq L}^{-1}$  and  $8.0 \text{ Bq L}^{-1}$ . These latter values were close to those found during the first campaign at the RV3 piezometer outside the site. During the third campaign, the hydrodynamic conditions on the site were the same as during the second campaign (pumping in operation). The piezometers near the Ouvèze

320 had low radon-222 values at about  $3.0 \pm 0.12 \text{ Bq L}^{-1}$  compared to  $11.0 \pm 0.24 \text{ Bq L}^{-1}$  at a downstream distance of 100 m away from the Ouvèze in the aquifer. During the first and the second campaigns, the radon-222 signatures for the Rhône were similar, and the same signature was observed for the Ouvèze during the first and third campaigns.



325 **Figure 4 : Radon-222 activity concentration as a function of the distance from the Rhône riverbank (Rhône at 0 m and Ouvèze at 750 m). The colors indicate the pumping state of the site (green for activated pumping, grey for stopped pumping)**

In comparison, the electrical conductivity of water samples measured during the second and third campaigns showed a similar behavior as radon-222 during pumping, with almost constant values in the aquifer at about  $680 \text{ mS cm}^{-1}$ , the Rhône at  $350 \text{ mS cm}^{-1}$  and the Ouvèze at  $570 \text{ mS cm}^{-1}$  (Figure 5). The wells and piezometers showed intermediate values between those observed in the aquifer and in the Rhône, with decreasing values for the wells and piezometers closer to the Rhône.



330

**Figure 5 : Electrical conductivity of groundwater and surface water as a function of the distance to the Rhône (Rhône at 0 m and Ouvèze River at 750 m).**

### 3.3 Stable isotopes of water

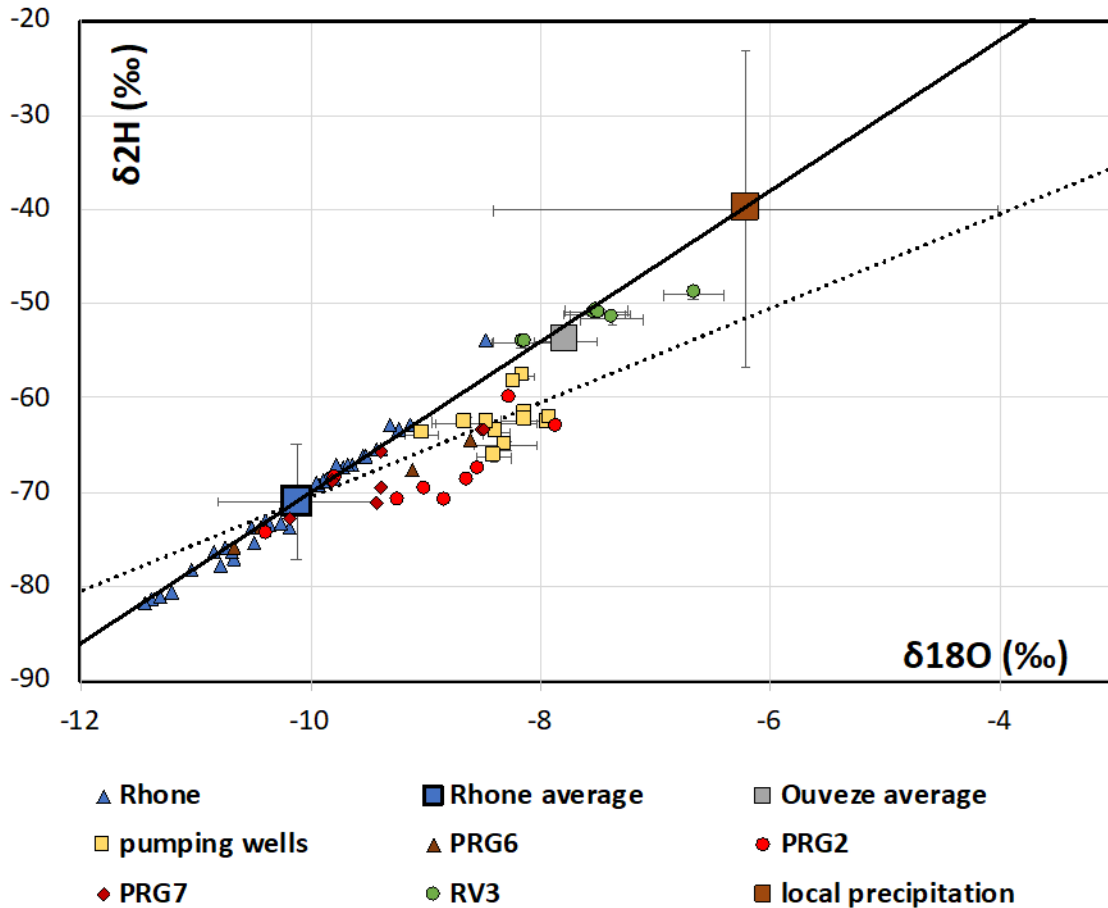
The two rivers delimiting the study area, the Rhône and the Ouvèze, present depleted isotopic compositions compared to local precipitation, attributed to the altitudes of their respective catchments (Figure 6). The groundwater isotopic compositions are spread around the global meteoric water line (GMWL), in the range of the composition of these two rivers, with a small influence of evaporation for some of the samples. As previously described, the sampling protocols were carefully implemented, and we are confident that the sample compositions were representative of the groundwater composition (sufficient purging phase for piezometers, and a continuous flux for pumped wells). The influence of a direct evaporation of groundwater is possible particularly at the riverbanks where the depth approaches zero and the particularly dry Mediterranean climate of the area (Coudrain-Ribstein et al., 1998). This effect is particularly relevant on the eastern side of the study area near the Ouvèze River, where, even at 150 meters from the river, the water table remains less than 2 meters below the surface, indicating a shallow depth over a significant portion of the area.

Considering the composition of local precipitation, the potential influence of a meteoric groundwater recharge remains undetectable. The piezometers located close to the Rhône (Prg: 42 m, Prg6: 33 m and Prg7: 35 m) present isotopic compositions fully compatible with a lateral recharge coming from the Rhône River, and further modified by the influence of evaporation. The spread of the data can be explained by the seasonal variation of the Rhône composition, and a variable contribution of evaporation.

The distances between the pumping wells and the Rhône River are slightly higher (P1 : 56 m, P2 : 58 m, P7a : 97 m), and their compositions are slightly enriched compared to that of these piezometers. This could be explained by a small contribution of the Ouvèze River, in addition to that of the Rhône. This will be discussed later.

350

On the other hand, the composition of the piezometer RV3, located in between the two rivers, points towards a dominant contribution of the Ouvèze River.



355 Figure 6 :Isotopic compositions of local precipitation (long term weighted average of the Avignon GNIP station), surface water (Rhône and Ouvèze rivers) and groundwater sampled in piezometers and pumping wells (average values of each sampling campaign). The Rhône’s isotopic data are obtained from (Poulain et al., 2021a). Error bars represent the standard deviations of average values. The black line represents the global meteoric water line. The dotted line represents a theoretical evaporation line crossing the Rhône average composition, and assuming a slope of 5.

360 **3.4 Interpretation of Temperature Periodic Signals**

Temperature monitoring over the same period showed a periodic variation at all wells and piezometers as well as in the Rhône. The variations in the piezometers showed a significant attenuation as well as a phase shift with respect to the Rhône River temperature signal. During the period when the pumping wells were stopped, discontinuities appeared in the data due to the change in the hydraulic regime. Temperature data for the pumping period can then be modeled using the 1D solutions

365 described in section 2.3 (Figure 7A).

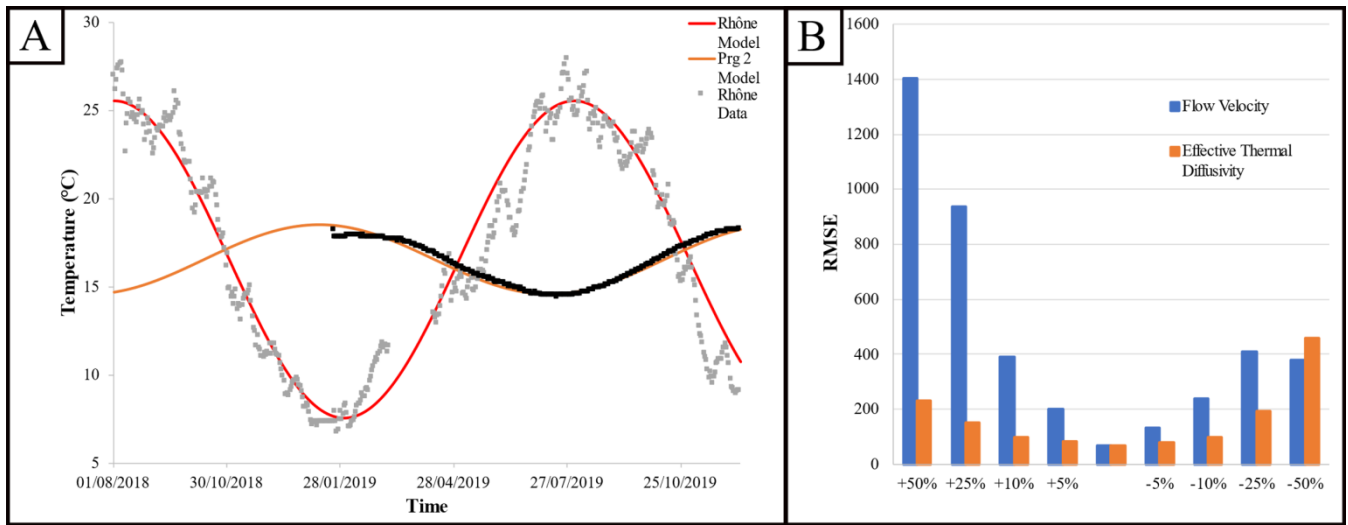


**Figure 7 : A) Temperature monitoring of piezometers Prg2 and the Rhône River and corresponding fitted 1D analytical expressions. B) Sensitivity analysis of Prg2 parameters**

Upon calibration, the 1D analytical expression for temperature provides the thermal front velocity and by extension the fluid  
 370 flow velocities. The pore velocity values between  $4.7 \cdot 10^{-6} \text{ m s}^{-1}$  and  $8.7 \cdot 10^{-6} \text{ m s}^{-1}$  were obtained with a porosity of 10% (value from the operator). The lower velocity was obtained for Prg1 while the three other piezometers led to velocities in the order of  $0.8 \cdot 10^{-5} \text{ m s}^{-1}$  (Table 1). The flow velocity appears as the more sensitive parameters, while the thermal diffusivity can vary to 10 % without impact the numerical result (Figure 7B). The flow velocity values are smaller than the first estimate made by calculating Darcy's flux based on the site hydraulic conductivity data (average value of  $1.3 \cdot 10^{-3} \text{ m s}^{-1}$ ) and the hydraulic head  
 375 gradient and leading to values ranging from  $1.10^{-4}$  to  $3.10^{-4} \text{ m s}^{-1}$ . This difference can be explained by the fact that the heat transport accounts for the entire continuum between the river and the aquifer with possible heterogeneity, while the Darcy method considers a homogeneous aquifer. Thus, the lower velocities obtained by this method can be explained by the presence of finer materials along the banks or a partial clogging of the riverbed, reducing the hydraulic conductivity.

**380 Table 1 : Calculated pore fluid velocity and thermal parameters based on the 1D periodic temperature analytical solution, and distance between the piezometers and the Rhône River**

| <i>Piezometers</i> | <i>Distance (m)</i> | <i>Pore velocity (m s<sup>-1</sup>)</i> | <i>Ke(m s<sup>-1</sup>)</i> |
|--------------------|---------------------|---|-----------------------------|
| <i>Prg2</i>        | 42                  | $8.71 \cdot 10^{-6}$                    | $7.29 \cdot 10^{-7}$        |
| <i>Prg7</i>        | 35                  | $6.75 \cdot 10^{-6}$                    | $8.44 \cdot 10^{-7}$        |
| <i>Prg6</i>        | 33                  | $8.10 \cdot 10^{-6}$                    | $5.13 \cdot 10^{-7}$        |
| <i>Prg1</i>        | 45                  | $4.67 \cdot 10^{-6}$                    | $5.34 \cdot 10^{-7}$        |



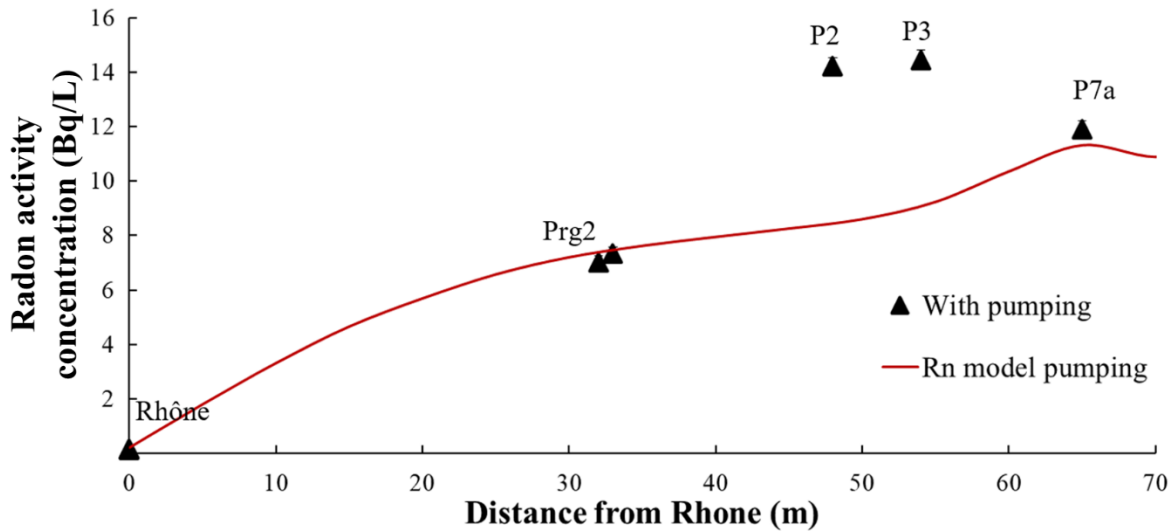
### 3.5 Fluid flow and transport modeling of the alluvial aquifer at the study site

#### 3.5.1 Fluid flow modeling and calibration

- 385 The hydraulic conductivity calibration consists in adjusting the values of the model to reproduce the measured piezometric levels. The PEST package was used to calibrate the model using the piezometric level during the site activity (pseudo-steady state). After calibration the model reproduce the groundwater level (RMSE=0.018 m) and provides hydraulic conductivity values between  $1.10^{-2}$  and  $1.10^{-4}$  m s<sup>-1</sup> for the aquifer and lower value of  $5.10^{-5}$  for the Rhone riverbank (values consistent with the operator reports).
- 390 Modeling under pumping conditions results in a calculated flow from the Ouvèze to the well field, as well as from the Rhône to the well field. In accordance with the piezometric monitoring, the piezometric depression is deeper in the southern part of the site during pumping. When pumping is active, the site is fed on the east side by the aquifer itself fed by the Ouvèze and on the west side directly by the Rhône (Figure 3A). Without pumping, the natural piezometric level is consistent with the piezometric monitoring during the pumping stop period with a reversal of the Rhône-aquifer exchange at the site. In fact, in
- 395 this configuration, the flow is uniformly directed from the Ouvèze to the Rhône, including at the extraction site (Figure 3B). The calibrated model allows to determine the water budget of the system with 56%of the water exploited at the pumping wells comes from the Ouvèze, 38% from the Rhône, and 6% from the recharge associated with rainfall.

#### 3.5.2 Radon-222 Transport Modelling

- Introducing the reactive transport of the radon-222 enables producing a profile of the aquifer from the Rhône to the well.
- 400 Figure 8 shows that the MT3D transport model accurately reproduced the observations obtained during the different campaigns under the same hydrodynamic conditions, with a gradual increase in radon-222 activity concentration in the aquifer during pumping, due to the progressive increase in radon-222 concentration in the water coming from the Rhône due to gas production within the aquifer. The radon-222 activity concentration increases to a maximum of about 12.0 Bq L<sup>-1</sup> at about 60 m of the Rhone River.



405

Figure 8 : Comparison between measured and simulated radon-222 activity concentrations in the Rhône River, piezometers and pumping wells in pumping conditions.

#### 4 Discussion

The groundwater is characterized by variable radon-222 activity concentrations between 8.0 Bq L<sup>-1</sup> and 15.0 Bq L<sup>-1</sup> which can be explained by some heterogeneity in internal radon-222 production due to petrographic variability. During the pumping period, the radon-222 measurement indicated groundwater recharge from both rivers, i.e., the Rhône and the Ouvèze, thus inducing low radon-222 activity concentrations during pumping. These supplies are confirmed by radon-222 in the piezometers near the Rhône and the Ouvèze, even if due to the progressive enrichment of radon-222 in the aquifer, the activity concentration returns to an equilibrium value in the order of 12.0 Bq L<sup>-1</sup> from 50 m downstream. As the wells are located between 50 and 90 meters of Rhône, at this distance the dilution effect of radon-222 activity concentration is no longer visible in the wells, contrary to the piezometers. For the Ouvèze, as for the Rhône riverbank, the lower radon-222 signal caused by the intrusion of the river water with a low radon-222 concentration disappears moving away from the river. We can deduce that the pumping wells producing the piezometric depression have a multiple supply with one part coming from the Rhône River and another one from the groundwater supplied by the Ouvèze. This hypothesis is supported by the piezometric contours that shows a flow from the Ouvèze towards the Rhône either in pumping or no pumping conditions. However, the radon-222 activity concentration does not allow for total quantification of recharge.

Our findings align with the work by Schubert et al. (2006), who also used radon-222 as a tracer to estimate the infiltration of surface waters into aquifers. Their study demonstrated that radon-222 is a valuable tool for identifying the movement of surface water into groundwater systems, particularly when the surface water has significantly lower radon-222 concentrations than groundwater. Similarly, we effectively traced the dilution of the radon-222 activity concentrations in the aquifer due to river water infiltration. The gradual return to equilibrium radon-222 concentrations further supports the idea of progressive radon-

425

222 enrichment as the river water moves through the aquifer. However, unlike Schubert et al., our study also considers the impact of pumping activities, which introduces additional complexity in interpreting radon-222 signals. This comparison highlights the versatility of radon-222 as a tracer and its applicability in various hydrological settings, including those influenced by anthropogenic activities like pumping.

The dual supply to the pumping wells is well supported by the  $\delta^{18}\text{O}$ - $\delta^2\text{H}$  data, which indicate a mixture of water from both the Rhône and the Ouvèze. The piezometers near the Rhône exhibit isotopic compositions consistent with lateral recharge from the Rhône, further modified by evaporation. In contrast, the isotopic compositions of the pumping wells are slightly enriched compared to those of these piezometers, suggesting an additional contribution from the Ouvèze. This is further confirmed by the isotopic composition of the piezometer RV3, located between the two rivers along the flow line from the Ouvèze, which indicates a dominant contribution from the Ouvèze.

In this first approach, the annual recharge due to rain was considered as negligible with a value at 300 mm by year for an area of 3 km<sup>2</sup> and a total pumping of 12000 m<sup>3</sup> d<sup>-1</sup>. Some piezometer and pumping well data points exhibit signs of evaporation. Water from the wells was collected via an access tap connected to the pumping system, while piezometer water was collected using a pump with a purge corresponding to 3 times the piezometer volume. On the measurement chronicle covering a seasonal cycle, the Rhône does not show an evaporative signal. Considering the estimation of the recharge, this evaporative signature could be due only for a small part to the recharge. This evaporative signature is therefore probably produced by direct evaporation from the aquifer in a Mediterranean climatic context, as the water table rises closer to the surface near the rivers, particularly at the riverbanks where the depth approaches zero (Gao et al., 2022). This effect could be more pronounced on the eastern side near the Ouvèze River, where, even at a distance of 150 meters from the river, the water table remains less than 2 meters below the surface.

Although the isotopic phase shift could theoretically be analyzed using Equation (4), the reliability of the seasonal signal in the aquifer is questionable due to evaporation and low sampling frequency. Nevertheless, this method could be generally applicable in alluvial plains under pumping conditions if a seasonal isotopic signal is present in the river. It offers a fast, cost-effective way to assess dispersivity (a weakly constrained variable in hydrogeology which is the dispersivity) using a natural tracer, especially where artificial tracers are not feasible due to the proximity to sensitive sites (industrial, urban).

The water supply to the alluvial aquifer by the Ouvèze, suggested by piezometric data, is then clearly confirmed by radon, isotopic data, with the radon-222 activity concentrations of the piezometers close to the Ouvèze showing a decrease in activity concentration, as for the Rhône, and a similar isotopic composition between the piezometer RV3 located outside the site (to the east) and the Ouvèze.

The use of a simple 1D solution for the temperature record allowed determining the flow velocities by numerical inversion by reproducing the records. Hence, based on three piezometers the pore velocity was found in the order of 10<sup>-5</sup> m s<sup>-1</sup>. After calibration using PEST, constrained by the piezometric levels monitoring, the numerical model reproduced the natural flow, i.e., with and without pumping, with velocities consistent with those deduced from temperature signal interpretation. The transport modeling of the radon-222 supports the feeding of the alluvial aquifer by the Ouvèze, as shown by the intrusion of

radon-depleted water sampled at the piezometers near the river, as well as the pumping of the site by the Rhône. Simulated groundwater balance analysis makes it possible to determine a full quantification of water supplied to the site's pumping systems. Regarding uncertainty, the groundwater balance validated by the Radon transport calculations is obtained by calibrating a steady-state flow simulation. This steady-state calculation depends on hydraulic conductivity and recharge.

465 Modeling uncertainty is primarily caused by the standard equifinality problem i.e., the fact that several permeability-recharge field "pairs" could lead to the same quality of result (agreement between simulated and observed piezometric levels). As recharge represents a small fraction of the groundwater balance (less than 10%), the equifinality problem is very limited here. Therefore, the calibrated permeability field (using measurements as initial guesses) is very robust in a context where the piezometry is largely controlled by the rivers stages used as prescribed boundary conditions. It is therefore difficult to carry

470 out a sensitivity analysis (and therefore an uncertainty analysis) that would consist in varying the permeability field, as this would severely degrade the agreement with the observed piezometric levels. Overall, and despite an unquantified but likely limited model uncertainty, the major part of the water exploited at the pumping wells is sourced from the Ouvèze (around 60%), with a significant portion also coming from the Rhône (around 40%), and a smaller contribution from local recharge associated with rainfall. This calculated groundwater budget is consistent with the isotopic analysis, confirming an important

475 contribution of the Ouvèze. The simulations confirm a clear vulnerability of the site with respect to possible contaminations from the Rhône and the Ouvèze. The Rhône is extremely close to the pumping wells and remains the main threat regarding potential contamination issues.

## 5 Conclusion

In this study, the ability of a multi-tracer approach to quantify groundwater-surface water exchanges in a riverside pumping context connected to the aquifer was investigated. The objective was to quantify the groundwater-surface water interactions at

480 the local scale using a set of tracers in order to obtain robust information to feed a numerical model. This river-aquifer exchange system was simulated using the MODFLOW model under natural and pumping conditions.

Radon-222 has been used to trace the entry of river water with low radon-222 activity concentration into the aquifer, thus diluting the natural signal of the aquifer. This rarely used method allows tracing the exchange from the river towards the

485 aquifer, whereas radon-222 is mainly used to determine the groundwater discharge into surface water bodies. This method enables identifying the entry of surface water until a distance from the riverbank of about 50 meters.

The 1D transport model, which uses a periodic input signal, allows to analyze the horizontal heat flux in the aquifer. An inversion using the temperature records from the piezometers allows quantification of the flow velocity and the effective thermal diffusivity of the aquifer. The combination of the piezometric, radon-222 and isotope monitoring showed that both the

490 Rhône and the Ouvèze rivers recharge the aquifer.

The hydrogeological modeling allowed reproducing the set of observations and to precisely determine the water balance at the pumping site with a dominant contribution from the Ouvèze (around 60%) and secondary from the Rhône (around 40%). This

water balance highlights the vulnerability regarding possible pollutants from the two rivers. It is interesting to note that it may appear somewhat counterintuitive that the smaller river makes greater contributions to the aquifer recharge than the larger river, and indeed the water management company held that belief before this study. Despite the lower contribution of the Rhône, the greater proximity represents an important risk due to the shorter time to reach the wells and therefore a lower chance of retention or degradation of pollutants.

Beyond our case study, this study confirms the great interest of the radon-222 tracer in the context of groundwater-surface water exchanges when piezometers close to the riverbank are available, whatever the direction of the exchange. The use of different natural tracers such as temperature, isotopes or other natural tracers allows for a more accurate estimation of the hydraulic parameter and the creation of a more robust model and is especially interesting where the use of artificial tracers is not an option. Integrated tracer-modeling studies can thus help improve the understanding of aquifer functioning and contribute to a sustainable exploitation strategy.

### **Author contribution**

J. Texier prepared the manuscript with contributions from all co-authors. J. Texier performed the MODFLOW model with contributions from J. Gonçalves. Field work and data acquisition performed by all co-authors. Isotopic data analysis performed by J. Texier and C. Vallet-Coulomb. Radon-222 data analysis performed by J. Texier and T. Stieglitz.

### **Competing interests**

The authors declare that they have no conflict of interest.

### **Acknowledgments**

The Agence de l'Eau Rhône-Méditerranée-Corse, the Syndicat Rhône-Ventoux and SUEZ are acknowledged for their financial support. The modeling software used is Processing MODFLOW X ver.

### **References**

- Anderson, M.P., 2005. Heat as a ground water tracer. *Ground Water* 43, 951–968. <https://doi.org/10.1111/j.1745-6584.2005.00052.x>
- Anibas, C., Buis, K., Verhoeven, R., Meire, P., Batelaan, O., 2011. A simple thermal mapping method for seasonal spatial patterns of groundwater-surface water interaction. *Journal of Hydrology* 397, 93–104. <https://doi.org/10.1016/j.jhydrol.2010.11.036>

- Bernard-Jannin, L., Sun, X., Teissier, S., Sauvage, S., Sánchez-Pérez, J.M., 2017. Spatio-temporal analysis of factors controlling nitrate dynamics and potential denitrification hot spots and hot moments in groundwater of an alluvial floodplain. *Ecological Engineering* 103, 372–384. <https://doi.org/10.1016/j.ecoleng.2015.12.031>
- Bertln, C., Bourg, A.C.M., 1994. Radon-222 and Chloride as Natural Tracers of the Infiltration of River Water into an Alluvial Aquifer in Which There Is Significant River/Groundwater Mixing. *Environmental Science and Technology* 28, 794–798. <https://doi.org/10.1021/es00054a008>
- 525 Binet, S., Joigneaux, E., Pauwels, H., Albéric, P., Fléhoc, C., Bruand, A., 2017. Water exchange, mixing and transient storage between a saturated karstic conduit and the surrounding aquifer: Groundwater flow modeling and inputs from stable water isotopes. *Journal of Hydrology* 544, 278–289. <https://doi.org/10.1016/j.jhydrol.2016.11.042>
- Boano, F., Demaria, A., Revelli, R., Ridolfi, L., 2010. Biogeochemical zonation due to intrameander hyporheic flow. *Water Resources Research* 46, 1–13. <https://doi.org/10.1029/2008WR007583>
- 530 Bravo, H.R., Jiang, F., Hunt, R.J., 2002. Using groundwater temperature data to constrain parameter estimation in a groundwater flow model of a wetland system. *Water Resources Research* 38, 28-1-28–14. <https://doi.org/10.1029/2000wr000172>
- Brookfield, A.E., Sudicky, E.A., 2013. Implications of Hyporheic Flow on Temperature-Based Estimates of Groundwater/Surface Water Interactions. *Journal of Hydrologic Engineering* 18, 1250–1261. [https://doi.org/10.1061/\(asce\)he.1943-5584.0000726](https://doi.org/10.1061/(asce)he.1943-5584.0000726)
- 535 Brunner, P., Simmons, C.T., Cook, P.G., 2009. Spatial and temporal aspects of the transition from connection to disconnection between rivers, lakes and groundwater. *Journal of Hydrology* 376, 159–169. <https://doi.org/10.1016/j.jhydrol.2009.07.023>
- Cable, J.E., Burnett, W.C., Chanton, J.P., Weatherly, G.L., 1996. Estimating groundwater discharge into the northeastern Gulf of Mexico using radon-222. *Earth and Planetary Science Letters* 144, 591–604. [https://doi.org/10.1016/s0012-821x\(96\)00173-](https://doi.org/10.1016/s0012-821x(96)00173-2)
- 540 2
- Calver, A., 2001. Riverbed Permeabilities: Information from Pooled Data. *Ground Water* 39, 546–553. <https://doi.org/10.1111/j.1745-6584.2001.tb02343.x>
- Cardenas, M.B., 2009. Stream-aquifer interactions and hyporheic exchange in gaining and losing sinuous streams. *Water Resources Research* 45, 1–13. <https://doi.org/10.1029/2008WR007651>
- 545 Caridroit, Y., 1968. Etude , géologique et hydrogéologique de la région d ' Avignon.
- Cecil, L.D., Green, J.R., 2000. Radon-222, in: *Environmental Tracers in Subsurface Hydrology*. Springer, pp. 175–194.
- Chapman, S.W., Parker, B.L., Cherry, J.A., Aravena, R., Hunkeler, D., 2007. Groundwater-surface water interaction and its role on TCE groundwater plume attenuation. *Journal of Contaminant Hydrology* 91, 203–232. <https://doi.org/10.1016/j.jconhyd.2006.10.006>
- 550 Chen, X., 2007. Hydrologic connections of a stream-aquifer-vegetation zone in south-central Platte River valley, Nebraska. *Journal of Hydrology* 333, 554–568. <https://doi.org/10.1016/j.jhydrol.2006.09.020>
- Clark, I., Fritz, P., 1997. The environmental isotopes. *Environmental isotopes in hydrogeology* 312.

- Close, M., Matthews, M., Burbery, L., Abraham, P., Scott, D., 2014. Use of radon to characterise surface water recharge to groundwater. *Journal of Hydrology* 53, 113–125.
- 555 Constantz, J., 2008. Heat as a tracer to determine streambed water exchanges. *Water Resources Research* 46, 1–20. <https://doi.org/10.1029/2008WR006996>
- Constantz, J., Stonestrom, D.A., 2003. Heat as a tracer of water movement near streams. US Geological Survey Circular 1–96.
- Cook, P.G., Lamontagne, S., Berhane, D., Clark, J.F., 2006. Quantifying groundwater discharge to Cockburn River, 560 southeastern Australia, using dissolved gas tracers <sup>222</sup>Rn and SF<sub>6</sub>. *Water Resources Research* 42, 1–12. <https://doi.org/10.1029/2006WR004921>
- Cook, P.G., Rodellas, V., Andrisoa, A., Stieglitz, T.C., 2018. Exchange across the sediment-water interface quantified from porewater radon profiles. *Journal of Hydrology* 559, 873–883. <https://doi.org/10.1016/j.jhydrol.2018.02.070>
- Corbett, D.R., Burnett, W.C., Cable, P.H., Clark, S.B., 1997. Radon tracing of groundwater input into Par Pond, Savannah 565 River Site. *Journal of Hydrology* 203, 209–227. [https://doi.org/10.1016/S0022-1694\(97\)00103-0](https://doi.org/10.1016/S0022-1694(97)00103-0)
- Coudrain-Ribstein, A., Prax, B., Talbi, A., Jusserand, C., 1998. Is the evaporation from phreatic aquifers in arid zones independent of the soil characteristics? *Comptes Rendus de l'Academie de Sciences - SerieIIa: Sciences de la Terre et des Planetes* 326, 159–165. [https://doi.org/10.1016/s1251-8050\(00\)89030-8](https://doi.org/10.1016/s1251-8050(00)89030-8)
- Cousquer, Y., Pryet, A., Atteia, O., Ferré, T.P.A., Delbart, C., Valois, R., Dupuy, A., 2018. Developing a particle tracking 570 surrogate model to improve inversion of ground water – Surface water models. *Journal of Hydrology* 558, 356–365. <https://doi.org/10.1016/j.jhydrol.2018.01.043>
- Cousquer, Y., Pryet, A., Flipo, N., Delbart, C., Dupuy, A., 2017. Estimating River Conductance from Prior Information to Improve Surface-Subsurface Model Calibration. *Groundwater* 55, 408–418. <https://doi.org/10.1111/gwat.12492>
- Craig, H., 1961. Isotopic variations in meteoric waters. *Science* 133, 1702–1703.
- 575 Delottier, H., Pryet, A., Dupuy, A., 2017. Why should practitioners be concerned about predictive uncertainty of groundwater management models? *Water Resources Management* 31, 61–73.
- Di Ciacca, A., Leterme, B., Laloy, E., Jacques, D., Vanderborght, J., 2019. Scale-dependent parameterization of groundwater–surface water interactions in a regional hydrogeological model. *Journal of Hydrology* 576, 494–507. <https://doi.org/10.1016/j.jhydrol.2019.06.072>
- 580 Doherty, J., 2004. PEST: Model independent parameter estimation. Fifth edition of user manual. Watermark Numerical Computing.
- Dugan, H.A., Gleeson, T., Lamoureux, S.F., Novakowski, K., 2012. Tracing groundwater discharge in a High Arctic lake using radon-222. *Environmental Earth Sciences* 66, 1385–1392. <https://doi.org/10.1007/s12665-011-1348-6>
- Dujardin, J., Anibas, C., Bronders, J., Jamin, P., Hamonts, K., Dejonghe, W., Brouyère, S., Batelaan, O., 2014. Combinaison 585 des techniques d'estimation des écoulements pour améliorer la caractérisation des interactions eau de surface-eau souterraine dans la rivière Zenne, Belgique. *Hydrogeology Journal* 22, 1657–1668. <https://doi.org/10.1007/s10040-014-1159-4>

- Ellins, K.K., Roman-Mas, A., Lee, R., 1990. Using  $^{222}\text{Rn}$  to examine groundwater/surface discharge interaction in the Rio Grande de Manati, Puerto Rico. *Journal of Hydrology* 115, 319–341. [https://doi.org/10.1016/0022-1694\(90\)90212-G](https://doi.org/10.1016/0022-1694(90)90212-G)
- Engelhardt, I., Piepenbrink, M., Trauth, N., Stadler, S., Kludt, C., Schulz, M., Schüth, C., Ternes, T.A., 2011. Comparison of  
590 tracer methods to quantify hydrodynamic exchange within the hyporheic zone. *Journal of Hydrology* 400, 255–266.  
<https://doi.org/10.1016/j.jhydrol.2011.01.033>
- Engel, M., Mischel, S., Quanz, S., Frei, S., Radny, D., Voelpel, R., & Schmidt, A. (2024). Localizing and quantifying groundwater-surface water interactions at different scales: A tracer approach at the River Moselle, Germany. *Hydrological Processes*, 38(5), e15118. <https://doi.org/10.1002/hyp.15118>
- 595 Fette, M., Kipfer, R., Schubert, C.J., Hoehn, E., Wehrli, B., 2005. Assessing river-groundwater exchange in the regulated Rhone River (Switzerland) using stable isotopes and geochemical tracers. *Applied Geochemistry* 20, 701–712. <https://doi.org/10.1016/j.apgeochem.2004.11.006>
- Fleckenstein, J.H., Krause, S., Hannah, D.M., Boano, F., 2010. Groundwater-surface water interactions: New methods and models to improve understanding of processes and dynamics. *Advances in Water Resources* 33, 1291–1295.  
600 <https://doi.org/10.1016/j.advwatres.2010.09.011>
- Gao, H., Ju, Q., Jiang, P., Yan, W., Wang, W., Fu, X., & Hao, Z. (2022). Estimation of Daily Evaporation from Shallow Groundwater Using Empirical Models with a Temperature Coefficient. *Journal of Hydrometeorology*, 23(11), 1759–1772. <https://doi.org/10.1175/JHM-D-22-0014.1>
- Gardner, W.P., Susong, D.D., Solomon, D.K., Heasler, H.P., 2011. A multitracer approach for characterizing interactions  
605 between shallow groundwater and the hydrothermal system in the Norris Geyser Basin area, Yellowstone National Park. *Geochemistry, Geophysics, Geosystems* 12, 1–17. <https://doi.org/10.1029/2010GC003353>
- Gat, J.R., Mazor, E., Tzur, Y., 1969. The stable isotope composition of mineral waters in the Jordan Rift Valley, Israel. *Journal of Hydrology* 7, 334–352. [https://doi.org/10.1016/0022-1694\(69\)90108-5](https://doi.org/10.1016/0022-1694(69)90108-5)
- Gerecht, K.E., Cardenas, M.B., Guswa, A.J., Sawyer, A.H., Nowinski, J.D., Swanson, T.E., 2011. Dynamics of hyporheic  
610 flow and heat transport across a bed-to-bank continuum in a large regulated river. *Water Resources Research* 47, 1–12. <https://doi.org/10.1029/2010WR009794>
- Ghysels, G., Anibas, C., Awol, H., Tolche, A.D., Schneidewind, U., Huysmans, M., 2021. The significance of vertical and lateral groundwater–surface water exchange fluxes in riverbeds and riverbanks: Comparing 1d analytical flux estimates with 3d groundwater modelling. *Water (Switzerland)* 13, 1–25. <https://doi.org/10.3390/w13030306>
- 615 Gilfedder, B.S., Frei, S., Hofmann, H., Cartwright, I., 2015. Groundwater discharge to wetlands driven by storm and flood events: Quantification using continuous Radon-222 and electrical conductivity measurements and dynamic mass-balance modelling. *Geochimica et Cosmochimica Acta* 165, 161–177. <https://doi.org/10.1016/j.gca.2015.05.037>
- Gonçalvès, J., Vallet-Coulomb, C., Petersen, J., Hamelin, B., Deschamps, P., 2015. Declining water budget in a deep regional aquifer assessed by geostatistical simulations of stable isotopes: Case study of the Saharan “Continental Intercalaire.” *Journal of Hydrology* 531, 821–829. <https://doi.org/10.1016/j.jhydrol.2015.10.044>  
620



- Goto, S., Matsubayashi, O., 2009. Relations between the thermal properties and porosity of sediments in the eastern flank of the Juan de Fuca Ridge. *Earth, Planets and Space* 61, 863–870. <https://doi.org/10.1186/BF03353197>
- Grapes, T.R., Bradley, C., Petts, G.E., 2005. Dynamics of river-aquifer interactions along a chalk stream: The River Lambourn, UK. *Hydrological Processes* 19, 2035–2053. <https://doi.org/10.1002/hyp.5665>
- 625 Hatch, C.E., Fisher, A.T., Revenaugh, J.S., Constantz, J., Ruehl, C., 2006. Quantifying surface water-groundwater interactions using time series analysis of streambed thermal records: Method development. *Water Resources Research* 42, 1–14. <https://doi.org/10.1029/2005WR004787>
- Hiscock, K.M., Grischek, T., 2002. Attenuation of groundwater pollution by bank filtration. *Journal of Hydrology* 266, 139–144. [https://doi.org/10.1016/S0022-1694\(02\)00158-0](https://doi.org/10.1016/S0022-1694(02)00158-0)
- 630 Hoehn, E., Von Gunten, H.R., 1989. Radon in groundwater: A tool to assess infiltration from surface waters to aquifers. *Water Resources Research* 25, 1795–1803. <https://doi.org/10.1029/WR025i008p01795>
- Jiang, Z., Xu, T., Mallants, D., Tian, H., Owen, D.D.R., 2019. Numerical modelling of stable isotope ( $2\text{H}$  and  $18\text{O}$ ) transport in a hydro-geothermal system: Model development and implementation to the Guide Basin, China. *Journal of Hydrology* 569, 93–105. <https://doi.org/10.1016/j.jhydrol.2018.11.065>
- 635 Keery, J., Binley, A., Crook, N., Smith, J.W.N., 2007. Temporal and spatial variability of groundwater-surface water fluxes: Development and application of an analytical method using temperature time series. *Journal of Hydrology* 336, 1–16. <https://doi.org/10.1016/j.jhydrol.2006.12.003>
- Konrad, C.P., 2006. Location and timing of river-aquifer exchanges in six tributaries to the Columbia River in the Pacific Northwest of the United States. *Journal of Hydrology* 329, 444–470. <https://doi.org/10.1016/j.jhydrol.2006.02.028>
- 640 Kraemer, T.F., Genereux, D.P., Kendall, C., McDonnell, J.J., 1998. Isotope tracers in catchment hydrology. Applications of uranium and thorium-series radionuclides in catchment hydrology studies, Amsterdam 679–722.
- Kurylyk, B.L., Irvine, D.J., Mohammed, A.A., Bense, V.F., Briggs, M.A., Loder, J.W., Geshelin, Y., 2018. Rethinking the Use of Seabed Sediment Temperature Profiles to Trace Submarine Groundwater Flow. *Water Resources Research* 54, 4595–4614. <https://doi.org/10.1029/2017WR022353>
- 645 Lamontagne, S., Leaney, F.W., Herczeg, A.L., 2005. Groundwater-surface water interactions in a large semi-arid floodplain: Implications for salinity management. *Hydrological Processes* 19, 3063–3080. <https://doi.org/10.1002/hyp.5832>
- Lautz, L.K., 2010. Impacts of nonideal field conditions on vertical water velocity estimates from streambed temperature time series. *Water Resources Research* 46, 1–14. <https://doi.org/10.1029/2009wr007917>
- Long, A.J., Putnam, L.D., 2004. Linear model describing three components of flow in karst aquifers using  $18\text{O}$  data. *Journal of Hydrology* 296, 254–270. <https://doi.org/10.1016/j.jhydrol.2004.03.023>
- 650 Lu, C., Chen, S., Jiang, Y., Shi, J., Yao, C., Su, X., 2018. Quantitative analysis of riverbank groundwater flow for the Qinhuai River, China, and its influence factors. *Hydrological Processes* 32, 2734–2747. <https://doi.org/10.1002/hyp.13219>
- Mayer, A., Graillot, D., Jolivet, J., 2018. Quantification des échanges eaux souterraines - rivière à l' aide du radon . Étude pilote appliquée à la Cèze.

- 655 McCallum, J.L., Cook, P.G., Berhane, D., Rumpf, C., McMahon, G.A., 2012. Quantifying groundwater flows to streams using differential flow gaugings and water chemistry. *Journal of Hydrology* 416–417, 118–132. <https://doi.org/10.1016/j.jhydrol.2011.11.040>
- Mcdonald, B.M.G., Harbaugh, A.W., 1988. Chapter A 1 A MODULAR THREE-DIMENSIONAL FINITE-DIFFERENCE GROUND-WATER. U.S. Geological Survey Open-File.
- 660 Morel-Seytoux, H.J., Mehl, S., Morgado, K., 2014. Factors influencing the stream-aquifer flow exchange coefficient. *Groundwater* 52, 775–781. <https://doi.org/10.1111/gwat.12112>
- Morel-Seytoux, H.J., Miller, C.D., Mehl, S., Miracapillo, C., 2018. Achilles' heel of integrated hydrologic models: The stream-aquifer flow exchange, and proposed alternative. *Journal of Hydrology* 564, 900–908. <https://doi.org/10.1016/j.jhydrol.2018.07.010>
- 665 Munz, M., Schmidt, C., 2017. Estimation of vertical water fluxes from temperature time series by the inverse numerical computer program FLUX-BOT. *Hydrological Processes* 31, 2713–2724. <https://doi.org/10.1002/hyp.11198>
- Musial, C.T., Sawyer, A.H., Barnes, R.T., Bray, S., Knights, D., 2016. Surface water-groundwater exchange dynamics in a tidal freshwater zone. *Hydrological Processes* 30, 739–750. <https://doi.org/10.1002/hyp.10623>
- Nofal, S., 2014. Etude du fonctionnement hydrodynamique de la nappe alluviale d'Avignon : impact de l'usage du sol sur  
670 les mécanisme de recharge.
- Opsahl, S.P., Chapal, S.E., Hicks, D.W., Wheeler, C.K., 2007. Evaluation of ground-water and surface-water exchanges using streamflow difference analyses. *Journal of the American Water Resources Association* 43, 1132–1141. <https://doi.org/10.1111/j.1752-1688.2007.00093.x>
- Perrin, J., Jeannin, P.Y., Zwahlen, F., 2003. Epikarst storage in a karst aquifer: A conceptual model based on isotopic data,  
675 Milandre test site, Switzerland. *Journal of Hydrology* 279, 106–124. [https://doi.org/10.1016/S0022-1694\(03\)00171-9](https://doi.org/10.1016/S0022-1694(03)00171-9)
- Poulain, A., Marc, V., Gillon, M., Cognard-Plancq, A.L., Simler, R., Babic, M., Leblanc, M., 2021a. Multi frequency isotopes survey to improve transit time estimation in a situation of river-aquifer interaction. *Water (Switzerland)* 13. <https://doi.org/10.3390/w13192695>
- Poulain, A., Marc, V., Gillon, M., Mayer, A., Cognard-Plancq, A.L., Simler, R., Babic, M., Leblanc, M., 2021b. Enhanced  
680 pumping test using physicochemical tracers to determine surface-water/groundwater interactions in an alluvial island aquifer, river Rhône, France. *Hydrogeology Journal* 29, 1569–1585. <https://doi.org/10.1007/s10040-021-02331-1>
- Rau, G.C., Andersen, M.S., McCallum, A.M., Acworth, R.I., 2010. Analytical methods that use natural heat as a tracer to quantify surface water-groundwater exchange, evaluated using field temperature records. *Hydrogeology Journal* 18, 1093–1110. <https://doi.org/10.1007/s10040-010-0586-0>
- 685 Ren, J., Cheng, J., Yang, J., Zhou, Y., 2018. A review on using heat as a tool for studying groundwater–surface water interactions. *Environmentalearth sciences* 77, 1–13.
- Rivière, A., Gonçalves, J., Jost, A., Font, M., 2014. Experimental and numerical assessment of transient stream-aquifer exchange during disconnection. *Journal of Hydrology* 517, 574–583. <https://doi.org/10.1016/j.jhydrol.2014.05.040>

- Rosenberry, D.O., Briggs, M.A., Delin, G., Hare, D.K., 2016. Combined use of thermal methods and seepage meters to efficiently locate, quantify, and monitor focused groundwater discharge to a sand-bed stream. *Water Resources Research* 52, 4486–4503. <https://doi.org/10.1002/2016WR018808>
- Rushton, K., 2007. Representation in regional models of saturated river-aquifer interaction for gaining/losing rivers. *Journal of Hydrology* 334, 262–281. <https://doi.org/10.1016/j.jhydrol.2006.10.008>
- Sadat-noori, M., Anibas, C., Andersen, M.S., Glamore, W., 2021. A comparison of radon , heat tracer and head gradient methods to quantify surface water - groundwater exchange in a tidal wetland ( Kooragang Island ,. *Journal of Hydrology* 598, 126281. <https://doi.org/10.1016/j.jhydrol.2021.126281>
- Schmidt, C., Conant, B., Bayer-Raich, M., Schirmer, M., 2007. Evaluation and field-scale application of an analytical method to quantify groundwater discharge using mapped streambed temperatures. *Journal of Hydrology* 347, 292–307. <https://doi.org/10.1016/j.jhydrol.2007.08.022>
- Schmidt, A., Gibson, J. J., Santos, I. R., Schubert, M., Tattrie, K., & Weiss, H. (2010). The contribution of groundwater discharge to the overall water budget of two typical Boreal lakes in Alberta/Canada estimated from a radon mass balance. *Hydrology and Earth System Sciences*, 14(1), 79-89.
- Schubert, M., Knoeller, K., Treutler, H. C., Weiss, H., & Dehnert, J. (2006). 222Rn as a tracer for the estimation of infiltration of surface waters into aquifers. *Radioactivity in the Environment*, 8, 326-334. [https://doi.org/10.1016/S1569-4860\(05\)080265](https://doi.org/10.1016/S1569-4860(05)080265)
- Schubert, M., Siebert, C., Knoeller, K., Roediger, T., Schmidt, A., & Gilfedder, B. (2020). Investigating groundwater discharge into a major river under low flow conditions based on a radon mass balance supported by tritium data. *Water*, 12(10), 2838. <https://doi.org/10.3390/w12102838>
- Schulze-Makuch, D., 2005. Longitudinal dispersivity data and implications for scaling behavior. *Ground Water* 43, 443–456. <https://doi.org/10.1111/j.1745-6584.2005.0051.x>
- S raphin, P., Vallet-Coulomb, C., Gon alv s, J., 2016. Partitioning groundwater recharge between rainfall infiltration and irrigation return flow using stable isotopes: The Crau aquifer. *Journal of Hydrology* 542, 241–253. <https://doi.org/10.1016/j.jhydrol.2016.09.005>
- Shanafield, M., Cook, P.G., 2014. Transmission losses, infiltration and groundwater recharge through ephemeral and intermittent streambeds: A review of applied methods. *Journal of Hydrology* 511, 518–529. <https://doi.org/10.1016/j.jhydrol.2014.01.068>
- Sharma, M.L., Hughes, M.W., 1985. Groundwater recharge estimation using chloride, deuterium and oxygen-18 profiles in the deep coastal sands of Western Australia. *Journal of Hydrology* 81, 93–109. [https://doi.org/10.1016/0022-1694\(85\)90169-6](https://doi.org/10.1016/0022-1694(85)90169-6)
- Shu, L., Chen, X., 2002. Simulation of water quantity exchange between groundwater and the Platte River water, central Nebraska. *Journal of Central South University of Technology* 9, 212–215. <https://doi.org/10.1007/s11771-002-0029-8>
- Sophocleous, M., 2002. Interactions between groundwater and surface water: The state of the science. *Hydrogeology Journal* 10, 52–67. <https://doi.org/10.1007/s10040-001-0170-8>

- Stallman, R.W., 1965. Steady one-dimensional fluid flow in a semi-infinite porous medium with sinusoidal surface temperature. *Journal of Geophysical Research* 70, 2821–2827. <https://doi.org/10.1029/jz070i012p02821>
- 725 Stellato, L., Petrella, E., Terrasi, F., Belloni, P., Belli, M., Sansone, U., Celico, F., 2008. Some limitations in using <sup>222</sup>Rn to assess river - Groundwater interactions: The case of Castel di Sangro alluvial plain (central Italy). *Hydrogeology Journal* 16, 701–712. <https://doi.org/10.1007/s10040-007-0263-0>
- Stieglitz, T.C., Cook, P.G., Burnett, W.C., 2010. Inferring coastal processes from regional-scale mapping of <sup>222</sup>Radon and salinity: Examples from the Great Barrier Reef, Australia. *Journal of Environmental Radioactivity* 101, 544–552. <https://doi.org/10.1016/j.jenvrad.2009.11.012>
- 730 Stieglitz, T.C., van Beek, P., Souhaut, M., Cook, P.G., 2013. Karstic groundwater discharge and seawater recirculation through sediments in shallow coastal Mediterranean lagoons, determined from water, salt and radon budgets. *Marine Chemistry* 156, 73–84. <https://doi.org/10.1016/j.marchem.2013.05.005>
- Surridge, B.W.J., Baird, A.J., Heathwaite, A.L., 2005. Evaluating the quality of hydraulic conductivity estimates from piezometer slug tests in peat. *Hydrological Processes* 19, 1227–1244. <https://doi.org/10.1002/hyp.5653>
- 735 Tang, Q., Kurtz, W., Schilling, O.S., Brunner, P., Vereecken, H., Hendricks Franssen, H.J., 2017. The influence of riverbed heterogeneity patterns on river-aquifer exchange fluxes under different connection regimes. *Journal of Hydrology* 554, 383–396. <https://doi.org/10.1016/j.jhydrol.2017.09.031>
- Trauth, N., Musolff, A., Knöller, K., Kaden, U.S., Keller, T., Werban, U., Fleckenstein, J.H., 2018. River water infiltration enhances denitrification efficiency in riparian groundwater. *Water Research* 130, 185–199. <https://doi.org/10.1016/j.watres.2017.11.058>
- 740 Vallet-Coulomb, C., Séraphin, P., Gonçalves, J., Radakovitch, O., Cognard-Plancq, A.L., Crespy, A., Babic, M., Charron, F., 2017. Irrigation return flows in a mediterranean aquifer inferred from combined chloride and stable isotopes mass balances. *Applied Geochemistry* 86, 92–104. <https://doi.org/10.1016/j.apgeochem.2017.10.001>
- 745 Winter, T.C., 1999. Relation of streams, lakes, and wetlands to groundwater flow systems. *Hydrogeology Journal* 7, 28–45. <https://doi.org/10.1007/s100400050178>
- Winter, T.C., Judson W. Harvey, Franke, O.L., Alley, W.M., 1999. *Ground Water: A Single Resource*.
- Woessner, W.W., 2000. Stream and fluvial plain ground water interactions: Rescaling hydrogeologic thought. *Ground Water* 38, 423–429. <https://doi.org/10.1111/j.1745-6584.2000.tb00228.x>
- 750 Xie, Y., Batlle-Aguilar, J., 2017. Limits of heat as a tracer to quantify transient lateral river-aquifer exchanges. *Water Resources Research* 53, 7740–7755. <https://doi.org/10.1002/2017WR021120>
- Xie, Y., Cook, P.G., Shanfield, M., Simmons, C.T., Zheng, C., 2016. Uncertainty of natural tracer methods for quantifying river-aquifer interaction in a large river. *Journal of Hydrology* 535, 135–147. <https://doi.org/10.1016/j.jhydrol.2016.01.071>
- Zheng, C., Hill, M.C., Cao, G., Ma, R., 2012. MT3DMS: Model Use, Calibration, and Validation. *Transactions of the ASABE* 55, 1549–1559. <https://doi.org/10.13031/2013.42263>
- 755

Zheng, C., Wang, P., 1999. MT3DMS: A modular three-dimensional multispecies transport model for simulation of advection, dispersion, and chemical reactions of contaminants in groundwater systems. Technical report, Waterways Experiment Station, US Army Corps of Engineers. A modular three-dimensional multi-species ... 239.

760 Zill, J., Siebert, C., Rödiger, T., Schmidt, A., Gilfedder, B. S., Frei, S., ... & Mallast, U. (2023). A way to determine groundwater contributions to large river systems: The Elbe River during drought conditions. *Journal of Hydrology: Regional Studies*, 50, 101595. <https://doi.org/10.1016/j.ejrh.2023.101595>